An Experimental and Numerical Study on Crystallization Analysis Fractionation (Crystaf)

Siripon Anantawaraskul,[1] *João B.P. Soares,**[2] *Paula M. Wood-Adams*[3]

[1] Department of Chemical Engineering, McGill University, 3610 University Street, Montreal, Quebec, Canada H3A 2B2
[2] Institute of Polymer Research, Department of Chemical Engineering, University of Waterloo, Waterloo, Ontario, Canada N2L 3G1
[3] Department of Mechanical and Industrial Engineering, Concordia University, 1455 de Maisonneuve Blvd. West, Montreal, Quebec, Canada H3G 1M8

Summary: Crystallization analysis fractionation (Crystaf) is a new technique used to estimate the chemical composition distribution (CCD) of semi-crystalline copolymers. In this study, the effect of chain microstructure and operation parameters on Crystaf profiles was investigated using a series of ethylene/1-hexene copolymers and their blends. The Crystaf profiles were also modeled via stochastic simulation based on the distribution of average ethylene sequence lengths.

Keywords: chemical composition distribution (CCD); crystallization analysis fractionation (Crystaf); microstructure; separation techniques

1. Introduction

Crystallization analysis fractionation (Crystaf) is a new alternative technique to temperature rising elution fractionation (Tref) for estimating chemical composition distribution (CCD) of semi-crystalline copolymers.[1-4] Several previous investigations have compared the CCD results obtained with Crystaf to the ones obtained with Tref and DSC.[1, 3, 5-6] The main advantage of Crystaf is that it provides results comparable to the ones from Tref with relatively shorter analysis time and, in addition, Crystaf is also easier to operate than Tref. Due to its advantages, Crystaf has been widely used not only for polymer characterization but also for developing structure-property relationships.[7-8]

Crystaf analysis involves a single-step solution crystallization process where polymer molecules precipitate under slow cooling rates according to their crystallizabilities. The polymer concentration in solution at each crystallization temperature is monitored during the analysis.

 DOI: 10.1002/masy.200450205

These crystallization profiles are then converted to CCD using a calibration curve that relates crystallization temperature and average comonomer content.[4, 9] Details on Crystaf operation can be found elsewhere in the literature.[1-4, 10-12]

In this work we shade some light on the fractionation mechanism of Crystaf by investigating how polymer molecular structures and fractionation conditions can affect Crystaf results. Average comonomer content and number average molecular weight are the two main structural parameters that can influence the crystallization process in Crystaf. The effect of these two parameters was studied separately in the first part of our experiments and was also modeled via stochastic simulation. Previous attempts to model Crystaf and Tref profiles applied Stockmayer's distribution,[12] broadening Stockmayer's distribution,[13] and Monte Carlo simulation.[11, 14-15] In this work we used stochastic models to simulate average ethylene sequence distribution for estimating Crystaf profiles. In the second part of our experimentals, Crystaf analysis at different cooling rates were performed in order to understand the effect of crystallization kinetics during fractionation.

2. Experimental

2.1 Material

All polymer samples involved in this study were prepared with single-site type catalysts and had narrow and unimodal CCDs. Two sets of ethylene/1-hexene copolymers were used for this investigation. The first set was used to study the effect of molecular weight on Crystaf. This set of samples was prepared by fractionating the parent resins according to molecular weight using a preparative fractionation apparatus (PREP, PolymerChar, Spain) in solvent/non-solvent mode. This ensured that the fractionated samples contained the same comonomer content and different molecular weights.

The second sample set was used to study the effect of comonomer content on Crystaf. This set was composed of a series of ethylene/1-hexene copolymers with similar molecular weights but with different levels of comonomer incorporation. Part of this set of samples was also used for the study of crystallization kinetics on Crystaf.

Tables 1 and 2 summarize the properties of the samples used in this investigation.

Table 1 Properties of fractionated samples for the study of molecular weight effect on Crystaf

Sample	Number average molecular weight (M_n)	Fractionated sample	Number average molecular weight (M_n)	Mole fraction of 1-hexene (CPP) [+]
A	36,097	A1	16,689	0.0127
		A2	28,415	0.0127
		A3	44,905	0.0127
		A4	73,195	0.0127
		A5	104,096	0.0127
B	35,153	B1	30,905	0.023
		B2	51,137	0.023
		B3	71,866	0.023
		B4	97,313	0.023
		B5	151,641	0.023
C	34,252	C1	22,944	0.032
		C2	32,110	0.032
		C3	39,468	0.032
		C4	67,124	0.032

[+] The mole fraction of 1-hexene in the fractionated samples is assumed to be equal to the one measured by C^{13} NMR for the parent samples, as the mole fraction of comonomer was reported to be almost constant and independent of chain length in case of samples synthesized with single site catalyst.[16]

Table 2 Properties of samples for the study of comonomer content and crystallization kinetic effects on Crystaf

Sample	Number average molecular weight (M_n)	Mole fraction of 1-hexene (CPP)	PDI
1	34,533	0.0420	2.16
2	34,252	0.0314	2.18
3	34,872	0.0232	2.16
4	36,291	0.0151	2.35
5	36,097	0.0121	2.43
6	37,165	0.0068	2.50

2.2 Crystaf analysis

Crystaf analysis was performed using a Crystaf model 200 manufactured by PolymerChar S.A. (Valencia, Spain). The polymer samples were dissolved in 1,2,4-trichlorobenzene (TCB) at a concentration of 0.4 mg/mL. During the dissolution step, the polymer solution was held at 160° C for 60 minutes. The temperature of the solution was then decreased to 90° C and held at that temperature for 45 minutes for stabilization. During the analysis, the solution was cooled down to 30° C with a constant cooling rate of 0.1° C/min. The concentration of the polymer in solution was monitored using the in-line infrared detector.

3. Monte Carlo simulation

Monte Carlo simulation was used to generate populations of copolymer chains having statistical properties similar to the ethylene/1-hexene copolymers that were synthesized with a single-site type catalyst. The two main parameters used in the simulation were the overall propagation probability (*PP*) and the comonomer propagation probability (*CPP*). While *CPP* can be measured directly for random copolymers (it is equal to the mole fraction of comonomer, *CC*, in the copolymer), *PP* has to be calculated from average chain length (r_n) as follows:

$$r_n = \frac{M_n}{M_{CO} \cdot CC + M_{MO} \cdot (1 - CC)} \tag{1}$$

$$PP = \frac{r_n - 1}{r_n} \tag{2}$$

where M_{CO} and M_{MO} are the molecular weights of comonomer and monomer, respectively.

The information on the distribution of the average ethylene sequence (*AvgES*) of the samples was then recorded from the simulated molecules. The Gibbs-Thompson equation was used to relate the *AvgES* with the crystallization temperature assuming that: (1) the lamella thickness is proportional to *AvgES*, and (2) thermodynamic equilibrium is achieved during crystallization in Crystaf.

For these conditions, the Gibbs-Thompson equation becomes:

$$T_C = \frac{T_S^0 (AvgES - \alpha)}{AvgES} - T_S \tag{3}$$

where T_C is the crystallization temperature, T_S^0 is the equilibrium dissolution temperature for an infinitely long crystallite, α is a constant related to the enthalpy of fusion, and T_S is the supercooling temperature proposed by Beigzadeh et al.[14]

By using this relationship, the *AvgES* distribution can be converted to Crystaf profiles. More information on the Monte Carlo algorithm used herein has been given in a previous publication.[11]

4. Effect of number average molecular weight (M_n)

Figure 1 shows the effect of the number average molecular weight on Crystaf profiles. As the molecular weight increases, the Crystaf profiles become narrower. Nieto et al.[17] reported

similar findings for sets of ethylene homopolymers with varying molecular weights. Notice that the model fits the data well for this set of resins.

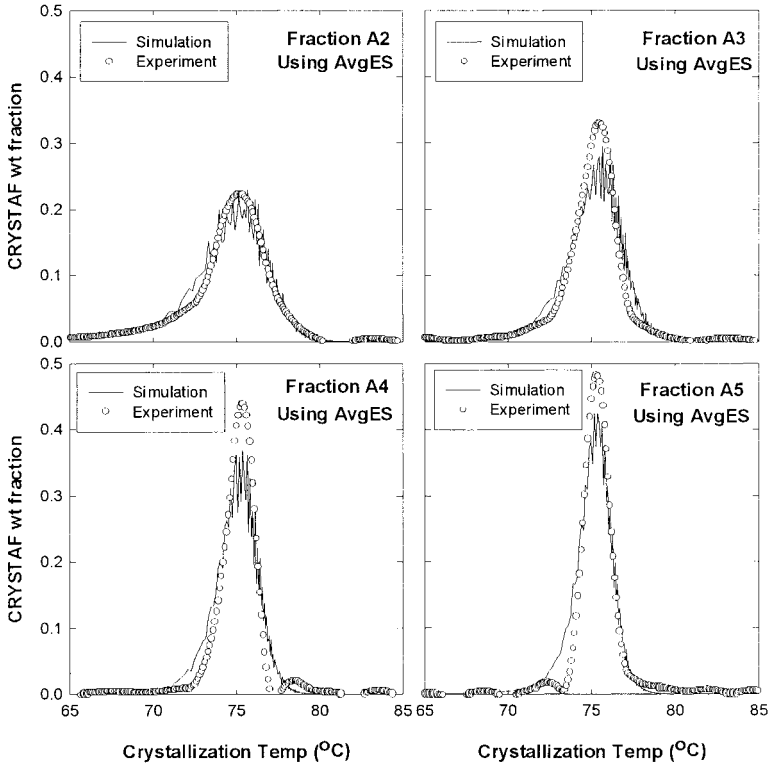

Figure 1. Effect of the number average molecular weight on Crystaf profiles

A slight increase in the Crystaf peak temperature is also be observed as the molecular weight increases. However, the shift in peak location is less than ± 1° C, which is well within the range of experimental error. Consequently, for all practical purposes, the effect of molecular weight on Crystaf peak location can be considered negligible.

5. Effect of average comonomer content

Comonomer content in the copolymer is the most important parameter affecting the crystallizability of ethylene/1-olefin copolymers. This is simply because comonomer units interrupt the regularity of the chain structure, thus lowering the crystallization temperature of the molecule. As the amount of comonomer incorporated into polymer chains increases, the crystallization temperature is lowered.

Figure 2 shows the effect of average comonomer content on Crystaf profiles (Sarzotti et al.[12]). Not only does the peak temperature decrease when comonomer content increases, but also the Crystaf distribution broadens significantly, in good agreement with the theory described by Stockmayer[12-13, 18] and well described by our stochastic simulations.

6. Effect of cooling rate

Although operating Crystaf in conditions approaching thermodynamic equilibrium would be preferable (as the effect of crystallization kinetics would be negligible), this is normally very difficult, if not impossible, to achieve because very long analysis times would be required. To investigate the effect of crystallization kinetics of Crystaf profiles, we compared the Crystaf analysis of several samples at various cooling rates.

Figure 3 shows the effect of cooling rate on Crystaf, indicating that the profiles are shifted to higher temperatures for slow cooling rates. This comes from the fact that polymer molecules are permitted to crystallize at high temperatures at a slow cooling rate, the condition closer to thermodynamic equilibrium. It is important to note that the typically used cooling rate of 0.1° C/min is far from the equilibrium, as lower cooling rates can still significantly shift the Crystaf profiles.

The effect of cooling rate on the Crystaf peak temperature is shown in Figure 4. An empirical linear relationship between the Crystaf peak temperature (T_P) and the natural logarithmic of the cooling rate (CR) was established:

$$T_P = a \times ln(CR) + b \tag{4}$$

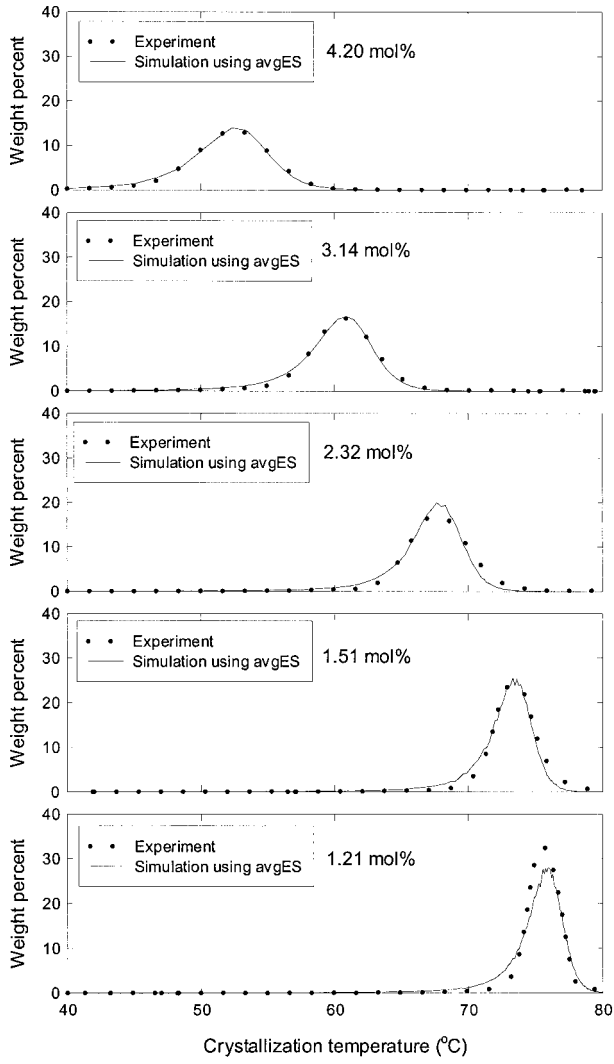

Figure 2. Effect of average comonomer content on Crystaf profiles

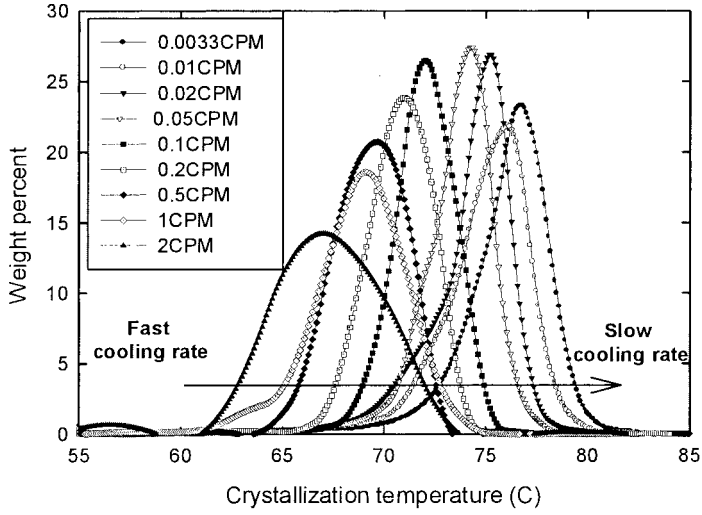

Figure 3. Effect of cooling rate on Crystaf profiles (sample 4 in Table 2)

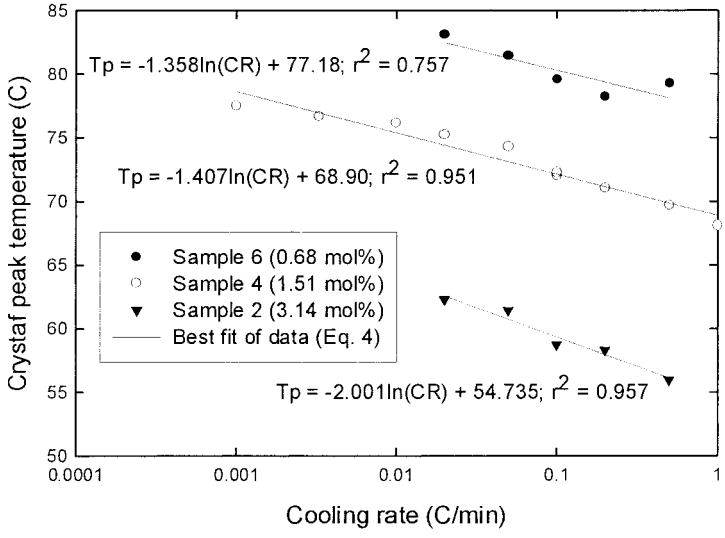

Figure 4. Crystaf peak temperature as a function of cooling rate

As the location of Crystaf peaks can vary significantly with the cooling rate, one should be careful when using calibration curves to estimate CCD. Using calibration curves produced from different cooling rates will over- or underestimates CCDs and average comonomer contents.

By combining the experimental data from this study and the ones from Sarzotti et al., we constructed a generalized calibration curve for ethylene/1-hexene copolymers for better estimation of average comonomer content over a range of cooling rates:

$$CC = 10 - 0.1216 \times T_P - 0.1653 \times ln(CR) \quad (5)$$

7. Cocrystallization

The possibility of cocrystallization during Crystaf analysis has been considered by many researchers.[1-2, 19-20] However, cocrystallization has not been reported as a significant factor, as most of the previous works considered only blends of different polymers (HDPE/LDPE/PP) or blends of polymers that contain very different crystallizabilities.

In this work, a blend of three ethylene/1-hexene samples was used for studying the cocrystallization phenomenon in Crystaf. The blend was prepared by mixing sample 2, 4, and 6 (see Table 2) at a weight ratio of 30:40:30. A strong cocrystallization effect was expected since the samples had relatively similar crystallizabilities. The information on cocrystallization at various cooling rates was obtained by comparing the experimental results for the blend with results calculated from the Crystaf analyses of each individual samples, assuming that there was no cocrystallization.

Figure 5 shows that cocrystallization plays an important role on the Crystaf analysis of this blend, especially for fast cooling rates. At a cooling rate of 0.5° C/min, the experimental Crystaf profile detects only a unimodal distribution, indicating a very strong cocrystallization effect. As slower cooling rates are used, the correct trimodal distribution is detected. However, even at the slowest cooling rate of 0.02° C/min, significant cocrystallization still takes place. At this slowest cooling rate, the deviation of experimental peak temperature seems to be higher than at a cooling rate of 0.05° C/min. However, this small deviation of peak temperature is within the range of experimental error.

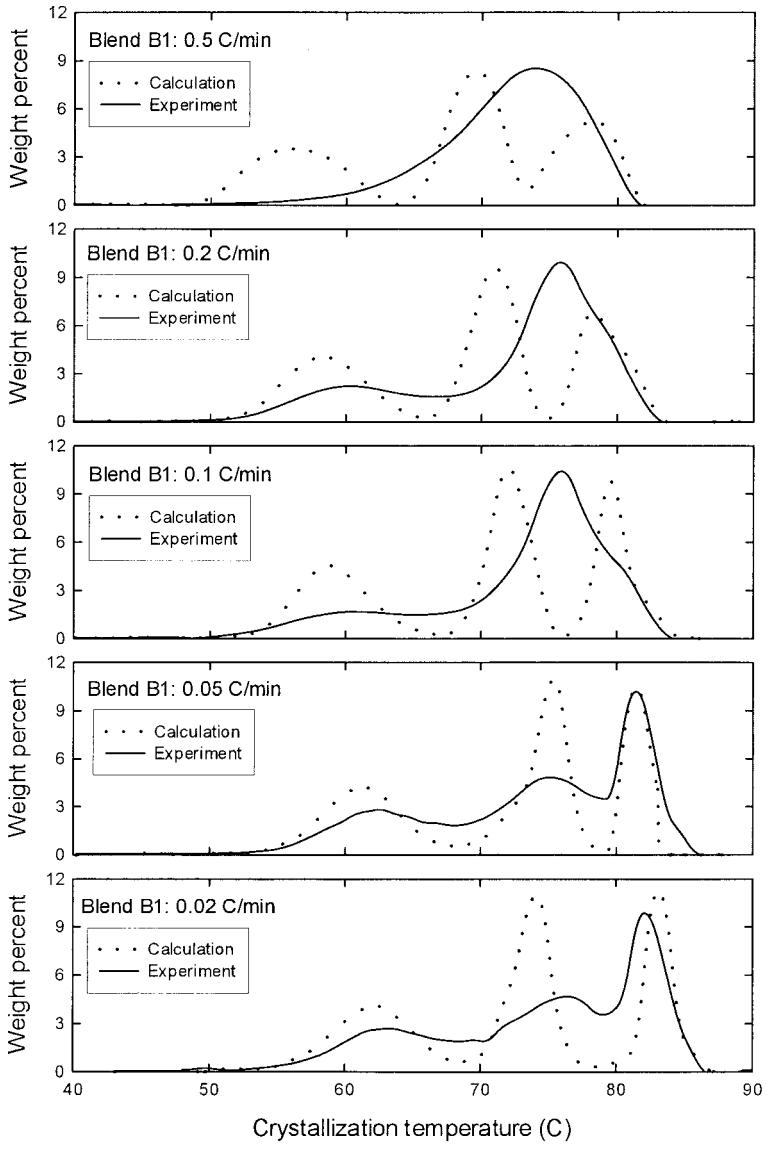

Figure 5. Comparisons between calculated and experimental Crystaf profiles at various cooling rates

It should be noted that at the cooling rate of 0.1° C/min, the typical cooling rate used in Crystaf analysis, strong cocrystallization could still be observed. Thus, this condition is not adequate for analyzing blends that are formed by individual samples having similar crystallization temperatures.

From Figure 5 at cooling rates of 0.2 and 0.1° C/min, it can be observed that the two chain populations at higher crystallization temperature seems to be more difficult to fractionate compared to a chain population at low crystallization temperature. This might be due to the fact that these two components have more similar chain crystallizabilities (smaller difference on peak temperatures). Similarity of chain crystallizability seems to be an important factor causing cocrystallization.

As cocrystallization in Crystaf can mislead the interpretation of CCD, it is important to understand this phenomenon in order to avoid it. Further work on the cocrystallization in Crystaf is under development in our group.

8. Conclusion

Crystaf is a powerful technique for estimating CCD of semi-crystalline copolymers. Although both molecular weight and average comonomer content affect Crystaf profile, average comonomer content is the only structural parameter that significantly influences the Crystaf peak temperature. Therefore, the estimation of the average comonomer contents with calibration curves using Crystaf peak temperatures seems to be adequate. However, since cooling rates can significantly influence Crystaf peak positions, one should be careful when using calibration curves reported in the literature for different cooling rates. A generalized calibration curve for ethylene/1-hexene random copolymers that takes into account the effect of cooling rate is proposed in the present study.

Cocrystallization affects the shape of Crystaf profiles for blends of samples that have similar crystallizabilities, especially at faster cooling rates. This fact should be taken into account when analyzing blends of copolymers with similar crystallizabilities or copolymers made with multiple site type catalysts such as heterogeneous Ziegler-Natta catalysts.

[1] B. Monrabal, *J. Appl. Pol. Sci.* **1994**, 52, 491.
[2] B. Monrabal, *Macromol. Symp.* **1996**, 110, 81.
[3] L.J.D. Britto, J.B.P. Soares, A. Penlidis, B. Monrabal, *J. Polym. Sci., Part B: Polym Phys.* **1999**, 37, 539.
[4] B. Monrabal, J. Blanco, J Nieto, J.B.P. Soares, *J. Polym. Sci., Part A: Polym. Chem.* **1999**, 37, 89.
[5] L.J.D Britto, J.B.P. Soares, A.Penlidis, *Polymer React. Eng.* **2000**, 8, 159.
[6] C. Gabriel, D. Lilge, *Polymer* **2001**, 42, 297.
[7] J.B.P. Soares, R.F. Abbott, J.D. Kim, *J. Polym. Sci., Part B: Polym. Phys.*, **2000**, 38, 1267.
[8] M. Gownder, *J. Plastic Film and Sheeting* **2001**, 17, 53.
[9] R. Brull, H. Pasch, H.G. Raubenheimer, R. Sanderson, A.J. van Reenen, U.M. Wahner, *Macromol. Chem. Phys.* **2001**, 202, 1281.
[10] S. Anantawaraskul, J.B.P. Soares, P.M. Wood-Adams, *J. Polym. Sci., Part B: Polym Phys.* **2003**, 41, 1762.
[11] S. Anantawaraskul, J.B.P. Soares. P.M. Wood-Adams, B. Monrabal, *Polymer* **2003**, 44, 2393.
[12] D.M. Sarzotti, J.B.P. Soares, A. Penlidis, *J.Polym. Sci., Part B: Polym Phys.* **2002**, 40, 2595.
[13] J.B.P. Soares, B. Monrabal, J. Nieto, J. Blanco, *Macromol. Chem. Phys.* **1998**, 199, 1917.
[14] D. Beigzadeh, J.B.P. Soares, T.A. Duever, *J. Appl. Pol. Sci.* **2001**, 80, 2200.
[15] S. Costeux, S. Anantawaraskul, P.M. Wood-Adams, J.B.P. Soares, *Macromol. Theory Simul.* **2002**, 11, 326.
[16] A. Faldi, J.B.P. Soares, *Polymer* **2001**, 42, 3057.
[17] J. Nieto, T. Oswald, F. Blanco, J.B.P. Soares, B. Monrabal, *J. Polym. Sci., Part B: Polym Phys.* **2001**, 39, 1616.
[18] S. Anantawaraskul, J.B.P. Soares, P.M. Wood-Adams, *Macromol. Theory Simul.* **2003**, 12, 229.
[19] H. Pasch, R. Brull, U. Wahner, B. Monrabal, *Macromol. Mater. Eng.* **2000**, 279, 46.
[20] R. Brull, V. Grumel, H. Pasch, H.G. Raubenheimer, R. Sanderson, U.M. Wahner, *Macromol. Symp.* **2002**, 178, 81.